crystals

MDPI

Article

Atomic Arrangement, Hydrogen Bonding and Structural Complexity of Alunogen, $Al_2(SO_4)_3 \cdot 17H_2O$, from Kamchatka Geothermal Field, Russia

Elena S. Zhitova [1,*], Rezeda M. Sheveleva [1,2], Andrey A. Zolotarev [1,3] and Anton A. Nuzhdaev [1]

[1] Institute of Volcanology and Seismology, Far East Branch of Russian Academy of Sciences, Piip Blvd. 9, 683006 Petropavlovsk-Kamchatsky, Russia; rezeda_marsovna@inbox.ru (R.M.S.); aazolotarev@gmail.com (A.A.Z.)
[2] Research Part of the Institute of Geosciences, Saint-Petersburg State University, University Emb., 7/9, 199034 Saint-Petersburg, Russia
[3] Crystallography Department, Saint-Petersburg State University, University Emb., 7/9, 199034 Saint-Petersburg, Russia
* Correspondence: zhitova_es@mail.ru

Abstract: Alunogen, $Al_2(SO_4)_3 \cdot 17H_2O$, occurs as an efflorescent in acid mine drainage, low-temperature fumarolic or pseudofumarolic (such as with coal fires) terrestrial environments. It is considered to be one of the main Al-sulphates of Martian soils, demanding comprehensive crystal-chemical data of natural terrestrial samples. Structural studies of natural alunogen were carried out in the 1970s without localization of H atoms and have not been previously performed for samples from geothermal fields, despite the fact that these environments are considered to be proxies of the Martian conditions. The studied alunogen sample comes from Verkhne–Koshelevsky geothermal field (Koshelev volcano, Kamchatka, Russia). Its chemical formula is somewhat dehydrated, $Al_2(SO_4)_3 \cdot 15.8H_2O$. The crystal structure was solved and refined to $R_1 = 0.068$ based on 5112 unique observed reflections with $I > 2\sigma(I)$. Alunogen crystalizes in the P-1 space group, $a = 7.4194(3)$, $b = 26.9763(9)$, $c = 6.0549(2)$ Å, $\alpha = 90.043(3)$, $\beta = 97.703(3)$, $\gamma = 91.673(3)$ °, $V = 1200.41(7)$ Å^3, $Z = 2$. The crystal structure consists of isolated SO_4 tetrahedra, $Al(H_2O)_6$ octahedra and H_2O molecules connected by hydrogen bonds. The structure refinement includes Al, S and O positions that are similar to previous structure determinations and thirty-four H positions localized for the natural sample first. The study also shows the absence of isomorphic substitutions in the composition of alunogen despite the iron-enriched environment of mineral crystallization. The variability of the alunogen crystal structure is reflected in the number of the "zeolite" H_2O molecules and their splitting. The structural complexity of alunogen and its modifications ranges from 333–346 bits/cell for models with non-localized H atoms to 783–828 bits/cell for models with localized H atoms. The higher values correspond to the higher hydration state of alunogen.

Keywords: alunogen; sulphate; geothermal field; Kamchatka; hydrated; crystal structure; hydrogen bonding; structural complexity; volcano

Citation: Zhitova, E.S.; Sheveleva, R.M.; Zolotarev, A.A.; Nuzhdaev, A.A. Atomic Arrangement, Hydrogen Bonding and Structural Complexity of Alunogen, $Al_2(SO_4)_3 \cdot 17H_2O$, from Kamchatka Geothermal Field, Russia. *Crystals* **2023**, *13*, 963. https://doi.org/10.3390/cryst13060963

Academic Editor: Carlos Rodríguez-Navarro

Received: 9 May 2023
Revised: 7 June 2023
Accepted: 9 June 2023
Published: 16 June 2023

1. Introduction

Alunogen is a hydrated aluminium sulphate with the formula $Al_2(SO_4)_3 \cdot 17H_2O$, regarded as a grandfather mineral species because it has been known since 1832 [1]. Alunogen is a rather widely distributed mineral reported as an acid mine drainage mineral and low-temperature fumarolic mineral or pseudofumarolic at coal fires [2–6]. The early study of its optical properties has shown that they considerably vary depending on the H_2O content in the mineral [7]. Rather detailed descriptions of alunogen crystal forms have been reported due to the Chilian mineralogical expedition of 1938 [8]. In this study [8], the authors found crystals of alunogen in small cavities where alums were dissolved and

noted that the true alunogen is colourless and triclinic, which readily dehydrated to white monoclinic mineral designated as meta-alunogen. The first crystal structure refinement of alunogen [7] was carried out on crystals from Grotta dell'Allume (or "Alum Cave"), Vulcano Island, Italy (symmetry and unit-cell parameters are given in Table 1), and enabled the determination of Al, S and O positions (two Al sites; three S sites and twenty-nine O sites). For clarity, we need to note that Grotta dell'Allume locality represented a tectonic cavity in the volcanic tuff in close proximity to the sea and on the island where the active Vulcano volcano (Italy) is located [9]. The conditions of the mineral formation there are more exotic than usual, because they include a mix of environments represented by a reaction of volcanic fluid with volcanic tuff in contact with sea water [9]. The first structural study of alunogen [6] confirmed the variation in the H_2O content and converged to the structural formula, $Al_2(SO_4)_3 \cdot 16.4H_2O$. The symmetry of the mineral (Table 1) and the position of the main atomic sites (for Al, S and O atoms) were confirmed via subsequent structural refinement, performed a couple of years later [10]. The refinement resulted in the formula $Al_2(SO_4)_3 \cdot 17H_2O$ [10]. The crystal structure of alunogen consists of isolated SO_4 tetrahedra and isolated $Al(H_2O)_6$ polyhedra (Figure 1) interconnected by hydrogen bonding. The H_2O molecules can be separated into two types: (i) those occurring in cavities and being of "zeolitic" nature (5 per formula unit); and (ii) those coordinating Al octahedra (12 per formula unit: 6 for each of two Al sites). In both studies, only oxygen atoms are localized for H_2O molecules. The crystal structure of alunogen is described [10] as consisting of pseudo-double sheets parallel to (010) alternating with a tetrahedra–water sheet composed of one SO_4 tetrahedra surrounded by H_2O molecules. This leads to perfect cleavage in the sheet stacking direction and formation of tabular crystals.

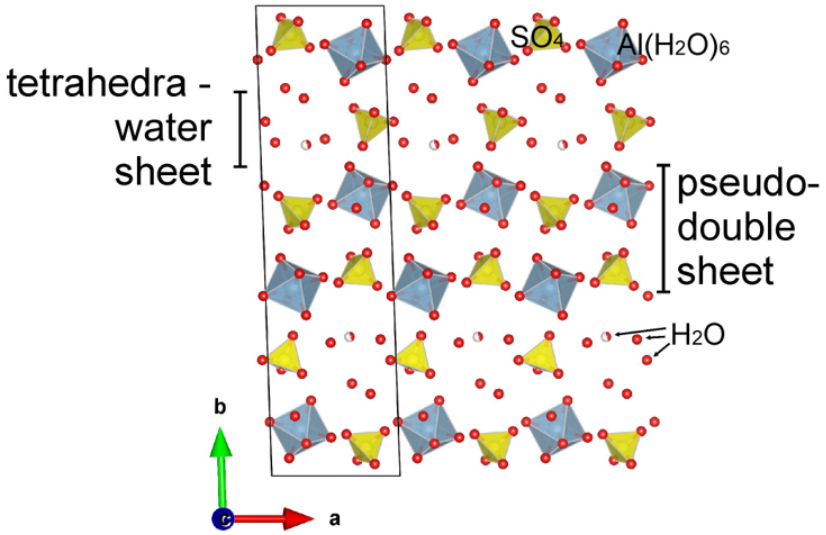

Figure 1. The crystal structure of alunogen obtained by [6].

Fang and Robinson [10] noted that O sites of H_2O molecules are restricted to 5, leading to 17 H_2O molecules (12 H_2O molecules coordinating Al and the other 5 H_2O "zeolite" molecules occurring in sulphate–water sheet) per formula unit. Then, the crystal structure of alunogen was obtained on synthetic material [11] and topologically verified with previous observations although the unit-cell setting was different, leading to the difference in the unit-cell parameters (Table 1). The crystal structure of synthetic material was supplemented by the localization of H atoms [11] but according to our analysis, the geometries of some H_2O molecules do not seem crystal-chemically reasonable. We also note that the selenate analogue of alunogen, $Al_2(SeO_4)_3(H_2O)_{16}$, was reported in the monoclinic space group $P2_1$ (Table 1) [12].

Assumptions that Al sulphates are one of the main minerals of Martian Al-bearing soils [13–16] triggered structure research of alunogen under low- and high-temperature

conditions and different moistures [17,18] carried out on synthetic samples. This research has shown that under Mars-relevant conditions (low temperature) alunogen undergoes a phase transition to low-temperature monoclinic modification (Table 1), while at a slightly elevated temperature of ~90 °C, partly dehydrated triclinic alunogen-like (or meta-alunogen) material with the formula $Al_2(SO_4)_3(H_2O)_{12}\cdot 1.8H_2O$ occurred (Table 1).

Table 1. Literature data on crystallographic parameters of alunogen and related phases obtained from alunogen upon cooling and heating.

	Alunogen	**Alunogen**	**Synthetic Analogue**	**Selenate Analogue**	**Low-Temperature Modification**	**Dehydrated Modification**
Chemical formula, $[Al(H_2O)_6]_2(TO_4)_3\cdot nH_2O$						
n, T	n = 4.4, T = S	n = 5, T = S	n = 4, T = S	n = 4, T = Se	n = 4.8, T = S	n = 1.8, T = S
Symmetry	Triclinic	Triclinic	Triclinic	Monoclinic	Monoclinic	Triclinic
Space group	*P*-1	*P*-1	*P*-1	$P2_1$	$P2_1$	*P*-1
a, Å	7.425	7.420	6.054	6.152	7.412	14.35
b, Å	26.975	26.970	7.424	27.445	26.834	12.49
c, Å	6.061	6.062	26.915	7.5650	6.078	6.09
α, °	90.03	89.57	88.047	90	90	92.66
β, °	97.66	97.34	89.948	97.93	97.31	96.65
γ, °	91.94	91.53	82.502	90	90	100.83
V, Å^3	1202.38	1202.73	1198.64	1265.09	1199.01	1062.8
Z	2	2	2	2	2	2
Genesis, locality	Natural from Vulcano, Italy	Natural from Königsber, Hungary	Synthetic	Synthetic	Colling of synthetic sample	Heating of synthetic sample
Reference	[6]	[10]	[11]	[12]	[17]	[18]

Thus, we can conclude that all previous structural studies carried out for natural and synthetic alunogen have shown the variability of the alunogen framework in relation to the number of "zeolite" H_2O molecules, as well as the possibility of changing the symmetry and unit-cell parameters of the mineral depending on the composition, mainly determined by the H_2O content, which presumably may even correspond not to alunogen but to its meta-forms. At the same time, alunogen is a common mineral in geothermal fields, which often acts as a proxy for Martian conditions. In particular, alunogen is widely distributed in the geothermal fields of Kamchatka [5,19–23], which is one of the most active volcanic areas in the world and belongs to the zone of the Pacific Ring of Fire. At the same time, the crystal structure of alunogen from geothermal fields worldwide or from Kamchatka has not been previously studied. Our work aims to fill this gap and analyse the crystal structure of natural alunogen from the standpoint of modern X-ray diffraction analysis.

2. Materials and Methods

2.1. Materials

In this study, we investigated the sample of alunogen collected from the surface of the Verkhne–Koshelevsky geothermal field associated with Koshelev volcano (South Kamchatka) (Figure 2a). South Kamchatka is part of the Kuril-Kamchatka Island arc system and characterized by high tectonic-magmatic activity, which is expressed on the surface by modern volcanism. The Verkhne–Koshelevsky geothermal field is located in the central part of the Koshelev volcanic complex (Figure 2b) in an erosion crater at absolute heights of 1200–1250 m. On the area of the field, especially in its northern part, large-block diluvial deposits are developed and, almost throughout the entire field area, argillic rocks

are widespread, which are the product of the hydrothermal transformation of basaltic andesites. Thermal manifestations are represented by steam-gas jets (Figure 2c), water–mud boilers, hot springs and lakes, and steaming ground. Thermal waters are characterized by temperatures of up to 95 °C, pH = 1.9–4.9, Eh = +60…+325 mV [24,25].

The sample was collected from the surface of 40 × 40 cm. The ground temperature of the sampling point was slightly elevated compared to the ground temperatures outside the geothermal area (retrospectively rated as ~40 °C) since the measured temperature at the depths of 30 cm was 80 °C. The sample was represented by a white polymineral efflorescent crust up to 1.5 cm thick (Figure 2d), composed of different hydrated sulphate minerals. In the crust, colourless tabular crystals of alunogen were separated using a binocular microscope and subjected to structure study. The associated minerals include Fe-Al and Fe sulphates: halotrichite, metavoltine and voltaite-group mineral. The efflorescent covered the pyrite-rich zone of the argillisites (Figure 2d). The descriptions of halotrichite from this locality were provided recently [22,23].

The main challenge of the efflorescent minerals study is in the small size and commonly low crystallinity that precluded previous structural reports. Additionally, even sample collection from hard-to-reach places (taking a few days using cars or on foot) associated with volcanic activity followed by accurate sampling and delivery of samples is also problematic. We were able to overcome these difficulties due to the experience of many years of field work in hard-to-reach places in Kamchatka.

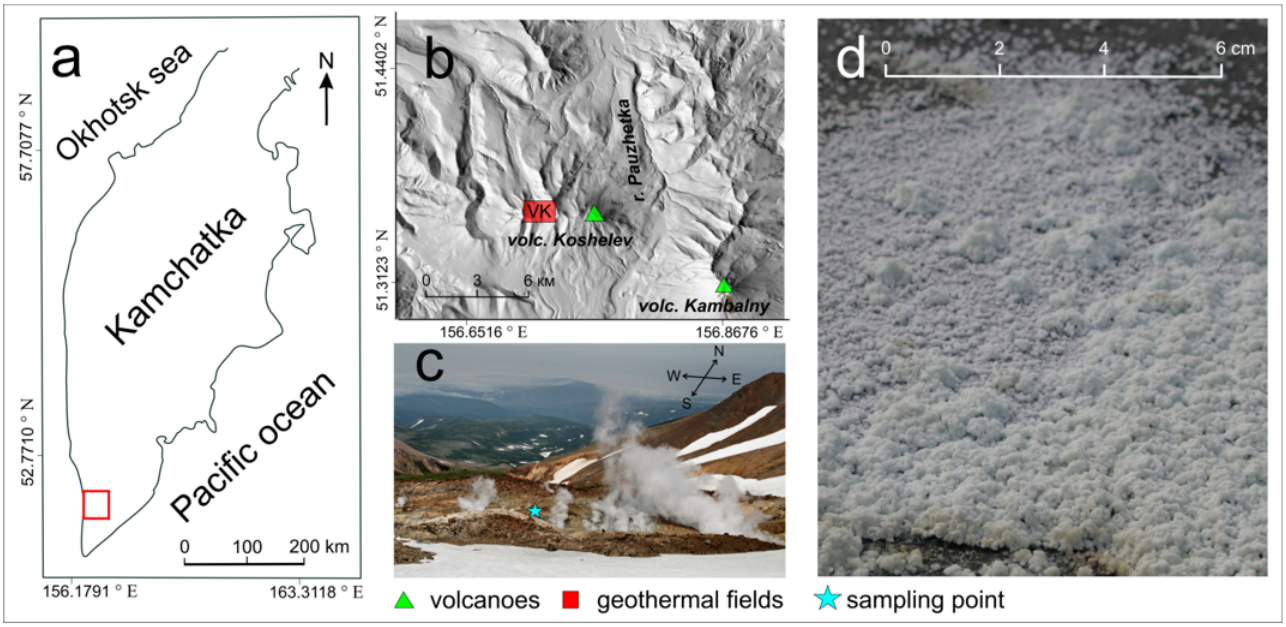

Figure 2. The place of the samples' collection: (**a**) the position of the Verkhne–Koshelevsky geothermal field on the map of Kamchatka; (**b**) the position of the Verkhne–Koshelevsky geothermal field relative to Koshelev and Kambalny volcanoes (both actve); (**c**) the general view to Verkhne–Koshelevsky geothermal field, steaming jets are visible; (**d**) the efflorescent polymineral crust composed of hydrated sulphates on the Verkhne–Koshelevsky geothermal field surface.

2.2. Methods

2.2.1. Scanning Electron Microscopy and Energy-Dispersive X-ray Spectroscopy

The chemical composition of alunogen was analysed at the "Geomodel" Resource Centre of the Scientific Park of St. Petersburg State University on a scanning electron microscope Hitachi S-3400N (Hitachi Ltd., Tokyo, Japan), equipped with an energy-dispersive spectrometer Oxford X-Max 20 (Oxford Instruments Ltd., Abingdon, UK), at an accelerating voltage of 20 kV, a probe current of 0.5 nA with various electron beam diameters of minimum 5 μm due to fast dehydration of alunogen under the electron beam. The

spectrometer was calibrated against a series of natural standards (MAC). The alunogen plates were deposited on carbon tape, carbon-coated and analysed via SEM and EDS. The previous studies of hydrated metal sulphates and fumarolic minerals have indicated the advantage of using the energy-dispersive mode instead of the wave-dispersive for their analysis [26–28] due to lower probe current and shorter time that it contributes to the preservation of material under study. In addition, energy-dispersive spectroscopy (EDS) enables the analysis of small-size grains of distinct minerals found in intimate association and in situ control of the sample condition during the spectrum acquisition.

2.2.2. Single-Crystal X-ray Diffraction

Single-crystal X-ray diffraction analysis was carried out for alunogen using a four-circle diffractometer Rigaku XtaLAB Synergy-S (Rigaku corporation, Akishima, Japan) operated with a monochromated Mo$K\alpha$ radiation (source: Mo$K\alpha$, λ = 0.71073 Å) at 50 kV and 1.0 mA and equipped with a CCD HyPix-6000HE detector (Rigaku corporation, Japan). The scan width was 1.0°, and the exposition time was 130 s. The long exposition time is due to extremely small crystal thickness and relatively weak diffraction. The CrysAlisPro [28] software package was used to process the data; an empirical absorption correction was calculated based on spherical harmonics implemented in the SCALES ABSPACK algorithm.

Numerous attempts were undertaken to collect single-crystal X-ray diffraction data of reasonable quality for structure refinement and hydrogen localization. These are because alunogen crystals are thin, maybe intergrown, twinned or low-crystalline. A photograph of the crystal on a nylon loop was taken during the analysis and given in the Supplementary file (Figure S1a), and one of the frames of collected single-crystal X-ray diffraction data is also presented in the Supplementary file (Figure S1b). The parameters of data collection are listed in Table 2.

Table 2. Crystal data, data collection, and structure refinement details for alunogen.

Crystal System	**Triclinic**
Space group	*P*-1
a (Å)	7.4194(3)
b (Å)	26.9763(9)
c (Å)	6.0549(2)
α (°)	90.043(3)
β (°)	97.703(3)
γ (°)	91.673(3)
V (Å^3)	1200.41(7)
Z	2
Calculated density (g/cm^3)	1.732
Absorption coefficient	0.496
Diffractometer	Rigaku XtaLAB Synergy-S
Temperature (K)	293
Radiation, wavelength (Å)	Mo$K\alpha$, 0.71073
Range of data collection, 2θ (°)	6.392–59.998
h, *k*, *l* ranges	−10→10, −37→37, −8→8
Total reflection collected	21,599
Unique reflections (R_{int})	6985(0.0408)
Number of unique reflections $F > 2\sigma(F)$	5112
Data completeness (%)	99.1
Refinement method	Full-matrix least-squares on F^2
Weighting coefficients a, b	0.0842, 4.2534
Data/ restrain/ parameters	6985/23/356
R_1 [$F > 2\sigma(F)$], wR_2 [$F > 2\sigma(F)$]	0.0680, 0.1830
R_1 all, wR_2 all	0.0947, 0.1981
Goodness-of-fit on F^2	1.049
Largest diff. peak and hole (ēÅ^{-3})	1.41/−0.62

The structure was solved and refined using the ShelX program package [29] incorporated into the Olex2 software shell [30] to R_1 = 0.068 based on 5112 unique observed reflections with $I > 2\sigma(I)$.

2.2.3. Structural Complexity

The structural complexity of alunogen and related phases were estimated using the approach of numerical evaluation of structural complexity developed by Krivovichev [31,32]. The complexity of crystal structure can be quantitatively characterized by the amount of Shannon information measured in bits (binary digits) per atom (I_G, bits/atom) and per unit cell ($I_{G,total}$, bits/cell), respectively, according to the following equations:

$$I_G = -\sum_{i=1}^{k} p_i \log_2 p_i \quad \text{(bits/atom)},$$

$$I_{G,total} = -v\, I_G = -v \sum_{i=1}^{k} p_i \log_2 p_i \quad \text{(bits/cell)},$$

where k is the number of different crystallographic orbits (independent crystallographic Wyckoff sites) in the structure and p_i is the random choice probability for an atom from the i-th crystallographic orbit, that is:

$$p_i = m_i/v,$$

where m_i is a multiplicity of a crystallographic orbit (i.e., the number of atoms of a specific Wyckoff site in the reduced unit cell), and v is the total number of atoms in the reduced unit cell. It is worth noting that the I_G value provides a negative contribution to the configurational entropy (S^{cfg}) of crystalline solids in accordance with the general principle that the increase in structural complexity corresponds to the decrease in configurational entropy [33]. Structural complexity was calculated using previously published crystal structure models (*cif*-files) listed in Table 1 and the program package ToposPro [34].

3. Results

3.1. Chemical Composition

The chemical composition of the alunogen sample is given in Table 3. The EDS spectra of alunogen show the presence of Al, S and O in its compositions. The contents of other elements with atomic numbers higher than that of C are below their detection limits. Alunogen dehydrates under vacuum conditions, which is manifested by the cracking of crystals and a decrease in water content, that is, an increase in the measured amount of Al_2O_3 and SO_3 oxides. The contents of Al_2O_3 and SO_3 oxides were measured. A direct measurement of H_2O content in our samples is not possible because alunogen is encountered in intergrowth with other hydrated sulphates and it is not possible to select a pure fraction for macro measurements. The H_2O content has been calculated taking into account the crystal structure data (see below). The analyses were normalized to 100 wt.%. The analyses (Table 3) show a good agreement with alunogen stoichiometry since Al:S ~ 2:3.

Table 3. Chemical composition of alunogen.

Constituent	Wt.%	apfu [1]
Al_2O_3	16.64	2.04
SO_3	37.88	2.96
H_2O	45.48	15.8
Total	100.00	-

[1] Atom per formula unit. Note: the chemical formula of the sample under study is $Al_2(SO_4)_3 \cdot 15.8H_2O$.

3.2. Crystal Structure

The obtained data were processed in a *P*-1 space group, a = 7.4194(3), b = 26.9763(9), c = 6.0549(2) Å, α = 90.043(3), β = 97.703(3), γ = 91.673(3) °, V = 1200.41(7) Å^3, Z = 2. Atom coordinates, site occupancies and isotropic displacement parameters are given in

Table 4. Selected bond lengths are listed in Table 5. The hydrogen bonding scheme is given in Table 6. Anisotropic displacement parameters are shown in the Supplementary file (Table S1). The crystallographic information file (cif) has been deposited via the joint Cambridge Crystal Data Centre CCDC/FIZ Karlsruhe deposition service.

Table 4. Atom coordinates, equivalent isotropic displacement parameters (Å^2) and site occupancies for alunogen.

Atom	x	y	z	U_{eq}	s.o.f. *
Al1	0.78185(17)	0.09886(4)	0.50210(19)	0.0167(2)	1
Al2	0.7633.8(17)	0.40035(4)	0.49664(19)	0.0152(2)	1
S1	0.26873(14)	0.06032(4)	0.01951(16)	0.0195(2)	1
S2	0.8767(2)	0.25246(5)	0.0304(2)	0.0373(3)	1
S3	0.25792(14)	0.43956(4)	0.01326(16)	0.018(2)	1
O1	0.7331(4)	0.07010(11)	0.2166(5)	0.0208(6)	1
H1A	0.629562	0.077332	0.129221	0.070(20)	1
H1B	0.726442	0.037102	0.203752	0.043(17)	1
O2	0.5469(4)	0.07816(12)	0.5602(5)	0.0253(6)	1
H2A	0.514433	0.077916	0.689613	0.038	1
H2B	0.484467	0.054801	0.490644	0.038	1
O3	0.8734(4)	0.03768(10)	0.6112(5)	0.0212(6)	1
H3A	0.987721	0.035292	0.677682	0.028(14)	1
H3B	0.798441	0.015192	0.663402	0.060(20)	1
O4	0.8327(5)	0.12538(11)	0.7909(5)	0.0242(6)	1
H4A	0.922831	0.112312	0.882852	0.060(20)	1
H4B	0.816461	0.155182	0.849011	0.036(16)	1
O5	0.6910(5)	0.15850(12)	0.3869(6)	0.0292(7)	1
H5A	0.755229	0.169346	0.289779	0.044	1
H5B	0.705253	0.180607	0.489091	0.044	1
O6	0.6723(5)	0.33977(12)	0.3726(5)	0.0269(7)	1
H6A	0.557522	0.333332	0.315609	0.060(20)	1
H6B	0.745632	0.320012	0.31037	0.080(30)	1
O7	0.5278(4)	0.41786(12)	0.5461(5)	0.0237(6)	1
H7A	0.477642	0.417182	0.672458	0.060(20)	1
H7B	0.445572	0.434082	0.450818	0.080(30)	1
O8	0.7227(4)	0.43029(11)	0.2133(5)	0.0212(6)	1
H8A	0.617753	0.423902	0.122989	0.024(13)	1
H8B	0.734013	0.462642	0.192039	0.032(15)	1
O9	0.8591(4)	0.46183(11)	0.6180(5)	0.0223(6)	1
H9A	0.975952	0.464422	0.681249	0.030(15)	1
H9B	0.782732	0.482812	0.667619	0.024(13)	1
O10	0.0003(4)	0.38597(12)	0.4492(5)	0.0241(6)	1
H10A	0.046469	0.359188	0.50095	0.036	1
H10B	0.028361	0.38766	0.317745	0.036	1
O11	0.0199(4)	0.11697(12)	0.4490(5)	0.0251(6)	1
H11A	0.068681	0.107622	0.328402	0.050(20)	1
H11B	0.041821	0.147012	0.507622	0.100(30)	1
O12	0.8036(4)	0.37269(11)	0.7830(5)	0.0228(6)	1
H12A	0.900811	0.385322	0.86682	0.040(17)	1
H12B	0.784091	0.341862	0.82899	0.049(19)	1
O13	0.1265(5)	0.09455(14)	0.0551(6)	0.0330(8)	1
O14	0.1975(5)	0.02533(13)	0.1607(6)	0.0344(8)	1
O15	0.3266(5)	0.03353(14)	0.2275(6)	0.0353(8)	1
O16	0.4281(5)	0.08828(13)	0.0448(5)	0.0279(7)	1
O17	0.0547(8)	0.2527(2)	0.0519(9)	0.0734(15)	1
O18	0.8967(7)	0.27314(17)	0.2560(8)	0.0571(13)	1
O19	0.7446(8)	0.28140(17)	0.1156(9)	0.0664(15)	1
O20	0.8074(8)	0.20139(14)	0.0374(7)	0.0581(14)	1
O21	0.4094(4)	0.41111(12)	0.0537(5)	0.0254(6)	1
O22	0.1939(5)	0.47437(12)	0.1653(6)	0.0323(8)	1

Table 4. *Cont.*

Atom	*x*	*y*	*z*	U_{eq}	s.o.f. *
O23	0.1077(5)	0.40518(13)	0.0516(5)	0.0280(7)	1
O24	0.3261(5)	0.46681(13)	0.2206(5)	0.0310(7)	1
Ow25	0.3442(10)	0.3054(3)	0.2757(17)	0.112(4)	0.938(19)
H25A	0.405511	0.284882	0.359081	0.168	0.938(19)
H25B	0.324039	0.29113	0.149356	0.168	0.938(19)
Ow26	0.2092(8)	0.32520(18)	0.7034(9)	0.0600(13)	1
H26A	0.253358	0.334482	0.83401	0.090	1
H26B	0.231035	0.29443	0.700003	0.090	1
Ow27	0.5093(9)	0.2186(3)	0.5909(12)	0.073(3)	0.828(16)
H27A	0.584529	0.235869	0.680159	0.109	0.828(16)
H27B	0.486283	0.193019	0.665419	0.109	0.828(16)
Ow28 **	0.1137(9)	0.2089(2)	0.5554(11)	0.0426(14)	0.65
H28A	0.071602	0.227891	0.450088	0.064	0.65
H28B	0.228548	0.213117	0.564612	0.064	0.65
Ow29 **	0.2236(18)	0.1790(5)	0.7460(20)	0.050(3)	0.35
H29A	0.3004	0.187195	0.659704	0.075	0.35
H29B	0.273149	0.188686	0.874557	0.075	0.35

* All occupancies are fixed since their refined occupancy is close to 100%, except for the O25 and O27 oxygen sites of H_2O molecules. ** O28 and O29 are disordered oxygen atoms of the one of the "zeolite" H_2O molecules.

Table 5. Selected bond lengths for alunogen.

Bond	Distance (Å)	Bond	Distance (Å)
Al–O1	1.880(3)	S1–O13	1.460(3)
Al1–O2	1.893(3)	S1–O14	1.475(3)
Al1–O3	1.889(3)	S1–O15	1.472(3)
Al1–O4	1.875(3)	S1–O16	1.480(3)
Al1–O5	1.862(3)	<S–O>	1.472
Al1–O11	1.888(3)		
<Al1–O>	1.881	S2–O17	1.473(5)
		S2–O18	1.462(4)
Al2–O6	1.868(3)	S2–O19	1.471(5)
Al2–O7	1.886(3)	S2–O20	1.459(4)
Al2–O8	1.888(3)	<S2–O>	1.467
Al2–O9	1.893(3)		
Al2–O10	1.871(3)	S3–O21	1.479(3)
Al2–O12	1.878(3)	S3–O22	1.472(3)
<Al2–O>	1.881	S3–O23	1.471(3)
		S3–O24	1.476(3)
		<S3–O>	1.475

Table 6. Hydrogen bonding scheme for alunogen.

D–H	*d*(D–H), Å	*d*(H⋯A), Å	<DHA, °	*d*(D⋯A), Å	A
O1-H1A	0.90	2.65	116.7	3.155(5)	O15
		1.74	177.1	2.640(4)	O16
O1-H1B	0.89	1.82	158.0	2.670(4)	O14
O2-H2A	0.85	1.83	169.7	2.674(4)	O16
O2-H2B	0.85	1.92	147.8	2.679(5)	O15
O3-H3A	0.89	2.85	121.7	3.402(4)	O13
		1.75	171.2	2.638(4)	O14
		2.93	100.8	3.221(6)	O3

Table 6. *Cont.*

D–H	*d*(D–H), Å	*d*(H⋯A), Å	<DHA, °	*d*(D⋯A), Å	A
O3-H3B	0.90	1.77	173.3	2.659(4)	O15
O4-H4A	0.89	1.79	170.5	2.678(5)	O13
		2.83	101.8	3.141(4)	O1
O4-H4B	0.90	1.70	161.1	2.561(5)	O20
O5–H5A	0.85	1.84	157.9	2.646(5)	O20
O5-H5B	0.85	1.97	125.4	2.557(7)	Ow27
		3.08	105.8	3.409(7)	Ow28
O6-H6A	0.89	1.72	160.1	2.572(8)	Ow25
O6-H6B	0.89	1.77	164.9	2.644(5)	O18
		2.78	134.2	3.460(7)	O19
O7-H7A	0.89	1.80	170.8	2.691(4)	O21
O7-H7B	0.90	1.80	166.1	2.683(4)	O24
O8-H8A	0.90	1.78	179.5	2.685(4)	O21
		2.62	117.3	3.136(5)	O24
O8-H8B	0.89	1.78	168.0	2.653(4)	O22
O9-H9A	0.90(1)	1.767(11)	172.0(14)	2.661(4)	O22
		2.837(14)	121.2(11)	3.392(4)	O23
		3.033(15)	102.7(11)	3.348(6)	O9
O9-H9B	0.89	1.78	167.4	2.657(4)	O24
O10-H10A	0.85	2.87	112.8	3.293(6)	O18
		1.86	151.2	2.640(6)	Ow26
O10-H10B	0.85	1.85	167.4	2.681(4)	O23
O11-H11A	0.90	1.80	168.3	2.685(4)	O13
O11-H11B	0.89	1.75	163.9	2.613(7)	Ow28
		2.02	136.7	2.729(12)	Ow29
O12-H12A	0.88	1.84	174.2	2.721(4)	O23
		3.11	101.5	3.397(6)	Ow26
O12-H12B	0.89	1.69	173.3	2.578(5)	O19
Ow25-H25A	0.85	2.36	166.7	3.190(13)	Ow27
Ow25-H25B	0.85	2.40	132.3	3.042(10)	O17
Ow26-H26A	0.85	2.39	128.1	2.991(6)	O21
		2.65	122.5	3.191(6)	O23
Ow26-H26B	0.85	2.38	108.1	2.769(7)	O17
		2.55	145.8	3.292(8)	Ow28
Ow27-H27A	0.85	1.99	174.7	2.841(8)	O19
		2.72	126.2	3.298(9)	O20
Ow27-H27B	0.85	2.10	120.4	2.631(14)	Ow29
Ow28-H28A	0.85	2.06	160.6	2.875(8)	O18
Ow28-H28B	0.85	2.07	176.4	2.918(9)	Ow27
Ow29-H29A	0.85	1.84	154.0	2.631(14)	Ow27
Ow29-H29B	0.85	2.48	99.3	2.752(15)	O17

The two Al sites, three S sites and twenty-nine O sites were localized from the difference Fourier maps and refined anisotropically. Site occupancies of Al, S, and O are given in Table 4 and they are all fully occupied with the exception of two oxygen positions (Ow25 and Ow27) of the "zeolite" H_2O molecules. The two-component twinning by matrix {−1 0 0 0 1 0 0 0 −1} was applied to the structure refinement. The hydrogen positions were localized from the difference Fourier maps for nine H_2O molecules of $Al(H_2O)_6$ octahedra or taking into account geometrical assumptions for other three H_2O molecules of $Al(H_2O)_6$ octahedra and for all four the "zeolite" H_2O molecules. In the first case, the O–H distances were softly restrained as 0.9 Å. Some of O···H and H···H distances were also softly restrained as 2.4–2.5 Å. All thirty-four H sites were located (Figure 3a) and refined isotropically with Ueq-values refined freely for H atoms of nine out of twelve H_2O molecules of $Al(H_2O)_6$ octahedra and using a riding model with Ueq-values restrained as 1.5 of donor O atom for H atoms of the other three H_2O molecules of $Al(H_2O)_6$ octahedra and for the all "zeolite" H_2O molecules. Additionally, one "zeolite" H_2O molecule is disordered and split into two partially occupied sites: Ow28 and Ow29 (Figure 3b) located at a distance of 1.56 Å with occupancies of 0.65 and 0.35, correspondingly.

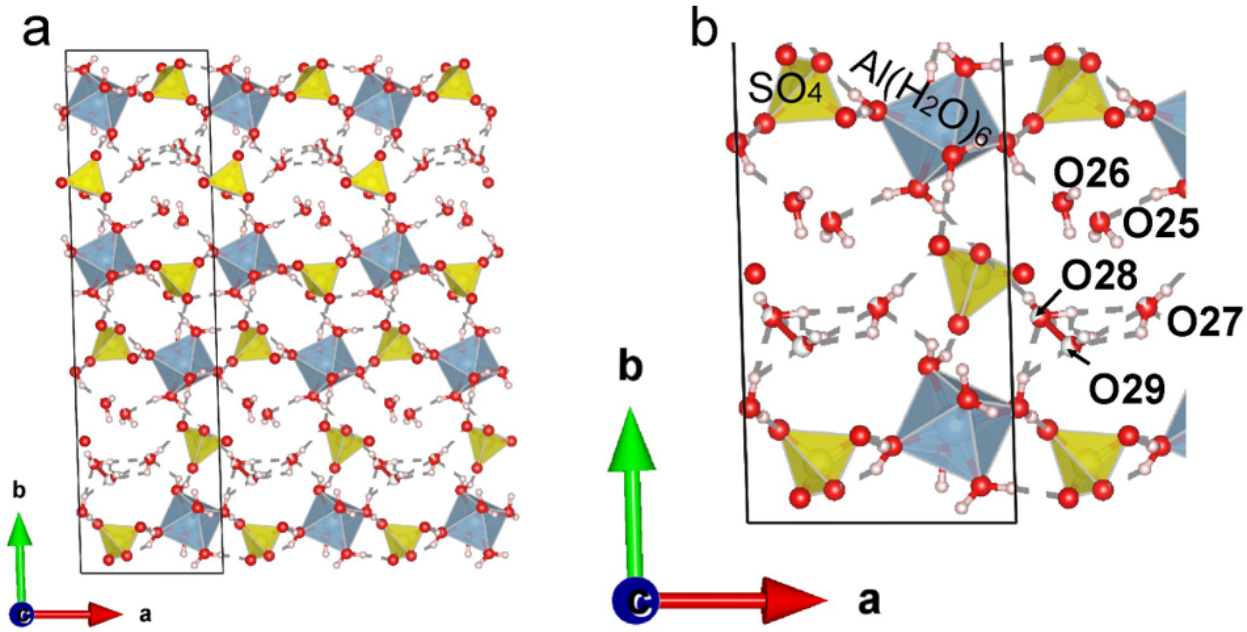

Figure 3. The crystal structure of alunogen obtained therein: (**a**) the framework showing H sites and hydrogen bonding scheme; (**b**) enlarged part showing labelling of the "zeolite" H_2O molecules and disordering of one of them producing two partially occupied sites: O28 and O29.

The hydrogen bonding scheme in the alunogen crystal structure is complex. The oxygen atoms labelled O1, O2…O12 coordinate Al1 and Al2 octahedra being donors (**D**) of two-centre hydrogen bonds [35]. The **D**–H bonds are in the range of 0.85–0.90 Å (Table 6). The oxygen atoms of the sulphate tetrahedra and the "zeolite" H_2O molecules act as an acceptor. For the case when the oxygen of the sulphate group is the acceptor (**A**), the following H···**A** distances are characteristically 1.70–1.92 Å and the **D**–H···**A** angles in the range of 147.8–179.5° (with averaged values of 1.79 Å and 167.9°, respectively). When the oxygen of the "zeolite" H_2O molecules is an acceptor, the H···**A** distances range from 1.72 to 2.02 Å and the **D**–H···**A** angles are in the range of 125.4–163.9° (with averaged values of 1.86 Å and 147.5°, respectively).

The oxygen atoms labelled Ow25, Ow26, Ow27 and Ow28 + Ow29 (split) belong to the "zeolite" H_2O molecules. For this type of H_2O molecule, the **D**–H bonds are ~0.85 Å. The oxygen atoms of SO_4 tetrahedra and the symmetrically independent "zeolite" H_2O molecules act as acceptors. In the case when the O atoms of SO_4 are acceptors, the H···**A**

distances range from 1.99 to 2.72 Å (with an average value of 2.37 Å) and the **D**–H···**A** angles are in the range of 108.1–174.7° (with an average value of 136.1°). When the oxygen of the "zeolite" H_2O molecules is an acceptor, the H···**A** distances range from 1.84 to 2.55 Å (an average value is 2.18 Å) and the **D**–H···**A** angles range from 120.4 to 176.4° (average value is 152.7°).

An analysis of the distribution of hydrogen bonds shows that stronger H···**A** bonds (Figure 4) are observed for H_2O molecules coordinating Al sites. At the same time, the sulphate group is a stronger acceptor resulting in a stronger hydrogen bond between the $Al(H_2O)_6$ octahedra and the SO_4 tetrahedra. The "zeolite" H_2O molecules are characterized by longer (and hence weaker) bonds with acceptors. Moreover, in the case of the "zeolite" H_2O molecule, a stronger hydrogen bond is formed with the other symmetrically independent "zeolite" H_2O molecules rather than SO_4 tetrahedra, leading to the formation of stronger hydrogen bonds between the "zeolite" H_2O molecules rather than its bonding with other structural units. In our opinion, that explains the possibility of alunogen dehydration and the possible formation of meta-alunogen.

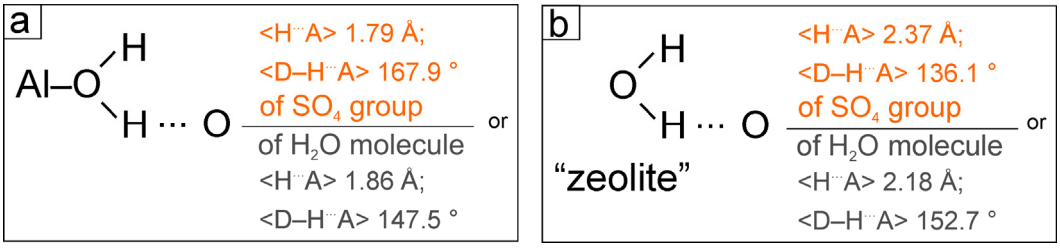

Figure 4. The average parameters of hydrogen bonding represented by H···**A** bonds and **D**–H···**A** angles of (**a**) $Al(H_2O)_6$ octahedra linked to SO_4 tetrahedra or the "zeolite" H_2O molecule and (**b**) the "zeolite" H_2O molecules linked to SO_4 tetrahedra or the symmetrically independent "zeolite" H_2O molecule.

3.3. Structural Complexity

The crystal structural complexity of alunogen and related phases is shown in Table 7. The parameters I_G and $I_{G,total}$ correspond to the complexity calculated for the structural models per atom and unit cell, respectively. Examination of the values in Table 7 shows their division into two groups: (i) I_G ~ 5.0–5.1 bits/atom and $I_{G,total}$ ~ 333–346 bits/cell and (ii) I_G ~ 6.0–6.1 bits/atom and $I_{G,total}$ ~ 783–828 bits/cell. Such a difference is due to the fact that earlier structure refinements do not contain H positions. Thus, hydrogen atoms contribute to more than half of structural complexity of alunogen, which is in line with the high hydration state of alunogen with ~ 45 wt.% of H_2O (Table 2). Table 7 also shows a direct correlation between the number of O sites corresponding to the "zeolite" H_2O molecules. For example, considering the crystal structures with non-localized H atoms, the complexity per unit cell is 333 bits/cell for selenate alunogen, with four O sites corresponding to the "zeolite" H_2O molecules and 346 bits/cell for natural alunogens with five fully or partly occupied O sites corresponding to the "zeolite" H_2O molecules. The same applies to the structures with localized H sites: the synthetic alunogen with n (number of the "zeolite" H_2O molecules) = 4 has a complexity per unit cell of 783 bits/cell, while low-temperature monoclinic modification with n = 4.8 has 828 bits/cell. In our structure refinement n = 3.8; however, one of the "zeolite" H_2O molecules is split into two with partial occupancy that leads to the identical complexities of our sample and low-temperature modification. This is also interesting to note that the transformation from triclinic to monoclinic symmetry is not outlined by a change in structural complexity. This is because the structure topology is preserved. We were unable to find a cif-file for dehydrated modification of alunogen. However, we can assume that it should have lower complexity since it has a lower content of the "zeolite" H_2O molecules.

Table 7. Crystal structure parameters and information complexities (I_G; $I_{G,total}$) of alunogen and related phases.

	Alunogen	**Alunogen**	**Alunogen**	**Synthetic Analogue**	**Selenate Analogue**	**Low-Temperature Modification**
Chemical formula, $[Al(H_2O)_6]_2(TO_4)_3 \cdot nH_2O$						
n, T	n = 3.8 [1], T = S	n = 4.4, T = S	n = 5, T = S	n = 4, T = S	n = 4, T = Se	n = 4.8, T = S
H-positions in cif-file	Located	Non-located	Non-located	Located	Non-located	Located
Symmetry	Triclinic	Triclinic	Triclinic	Triclinic	Monoclinic	Monoclinic
Space group	*P*-1	*P*-1	*P*-1	*P*-1	$P2_1$	$P2_1$
I_G, bits/atom	6.1	5.1	5.1	6.0	5.0	6.1
$I_{G,total}$ bits/cell	828	346	346	783	333	828
Reference	This research	6	10	11	12	17

[1] one position of the "zeolite" H_2O molecule is disordered and split to O28 and O29.

4. Discussion

In our study, the alunogen sample comes from a Fe-rich (both ferric and ferrous) environment and is found in intimate association with other Fe or Fe-Al hydrated sulphates. At the same time, Fe^{3+} does not incorporate into the crystal structure of alunogen studied therein. Following the ideas of Fang and Robinson [10], we conclude that the difference in the ionic size and polarization power should be responsible for that rather than the non-availability of Fe^{3+}. We can assume that even if some (limited) Al to Fe^{3+} substitution occurs in individual alunogen crystals, it should have a negative effect on the crystallinity of the alunogen precluding its structural study. It is interesting to note that according to our data, limited Al to Fe^{3+} substitution occurred in other hydrated sulphates from geothermal fields: alums and alunite/jarosite-group minerals where the formation of Fe^{3+}- or Al-dominant species in intimate association was observed rather than their full solid solution series [21] and halotrichite where Al site was free of impurities or contained limited Fe^{3+} [22,23]. If terrestrial geothermal fields are indeed a proxy for Martian conditions, then there should not only be iron sulphates, already well known for Mars, but also aluminium sulphates, and it can be assumed that alunogen or its modifications may be widespread (following mineral formation at geothermal fields). The alunogen described in this work contains the smallest amount of the "zeolite" H_2O molecules (3.8 *apfu* vs. 4–5 *apfu*) among structurally characterized natural and synthetic minerals. Despite the structural study of alunogen, including low- and high-temperature modifications [17,18], the question seems to be open on whether alunogen with different content of the "zeolite" H_2O molecules will behave identically under low-temperature conditions that are modelling Martian environments?

In this work, we provide modern crystal structure refinement of alunogen including the first localization of thirty-four hydrogen sites. Each of the Al and S sites has shown 100% occupancy. The structure consists of isolated $Al(H_2O)_6$ octahedra, SO_4 tetrahedra and the "zeolite" H_2O molecules that are connected to the three-dimensional network by hydrogen bonds. The hydrogen atoms form two-centre hydrogen bonds of $Al(H_2O)_6$ octahedra and the "zeolite" H_2O molecules. Four sites corresponding to the "zeolite" H_2O molecules were localized (including O and H atoms) with one "zeolite" H_2O molecule being disordered and split. Analysis of the hydrogen bonding network explains the possibility of alunogen dehydration since the independent "zeolite" H_2O molecules form stronger hydrogen bonding with each other rather than with other acceptors. The detailed information on the hydrogen bonding network should be helpful for band assignments in the vibration spectra of alunogen and its modifications that are in demand in connection with studies of Martian mineralogy by rovers and the development of remote and express methods of terrestrial minerals identification [2]. In general, the crystal structure of alunogen shows

variability only in the content of the "zeolite" H_2O molecules outlined by the consistency of the unit-cell volume (Tables 1 and 2) that can possibly be regarded as structure inflexibility towards isomorphic substitution.

Hydrogen sites contribute significantly to the structural complexity of alunogen increasing structural complexity per unit cell from 346 to 828 bits/cell. An increase in structural complexity by a factor of two or more due to hydrogen positions is also characteristic of other hydrated sulphates occurring in association with alunogen [22]. This is because the crystal structure of alunogen and other hydrated sulphates from the same association (e.g., halotrichite, alum-group minerals [22,35]) is built of isolated units (octahedra, tetrahedra and H_2O molecules) connected by hydrogen bonds. As suggested previously, highly hydrated minerals are good candidates for a better understanding of ionic species existing in solution [10]. In general, low polymerization of structural units is characteristic of the main efflorescent minerals growing from hydrothermal solution, including alunogen. Taking into account the abundance of alunogen at geothermal fields and recent experiments of transformation of alunogen to meta-alunogen at 40–80 °C [17], we consider the possibility of meta-alunogen occurrence at geothermal and/or fumarole fields is high despite the questionable mineral status of meta-alunogen.

We see a further perspective for the study of alunogen in the structural study of samples taken under different formation conditions. It would be especially interesting, in our opinion, to study alunogen crystallizing at a higher temperature in order to identify the relationship between the number of "zeolite" H_2O molecules and the crystallization temperature, which can lead to the findings of meta-alunogen; however, such work is very painstaking and would, most likely, need to be developed over many years, taking into account the complexity of the material.

5. Conclusions

We consider the crystal structure study of alunogen from the Verkhne–Koshelevsky geothermal field to be an important outcome for the characterization of naturally occurring highly hydrated sulphate minerals and their possible modifications. The chemical specificities of alunogen from the geothermal field are the absence of impurities (including Fe^{3+} despite $Fe^{2+,3+}$-rich environment) and lower H_2O content in comparison to previously structurally characterized natural and synthetic alunogens. From the structural point of view, the alunogen studied in this work is isotypic to previously reported structures of alunogen. However, in addition to previous studies, we were able to localize hydrogen atoms and characterize the complex hydrogen bonding network of the mineral. These data may be helpful for the detailed assignment of band positions in the vibrational spectra and useful for Mars mineralogical missions. Hydrogen atoms increase structural complexity per unit cell by more than two times, similar to other highly hydrated sulphates, which were found in association with alunogen. Combining the recently obtained experimental data on the transition of alunogen to meta-alunogen at a temperature of ~40–80 °C and our field temperature measurements at geothermal and fumarole fields, we assume that the findings of meta-alunogen under low-temperature volcano-related conditions are very likely. At the same time, the structural study of alunogen from the geothermal fields can be a starting point in the search and characterization of meta-alunogen or its possible structural varieties in nature.

Supplementary Materials: The following supporting information can be downloaded at: https://www.mdpi.com/article/10.3390/cryst13060963/s1, Figure S1: Photo of the crystal on a nylon loop (a) and single frame of collected single-crystal X-ray diffraction data; Table S1: Anisotropic displacement parameters ($Å^2$) for alunogen.

Author Contributions: Conceptualization, E.S.Z. and R.M.S.; methodology, R.M.S.; software, E.S.Z., R.M.S., A.A.Z. and A.A.N.; validation, E.S.Z., R.M.S., A.A.Z. and A.A.N.; formal analysis, E.S.Z., R.M.S. and A.A.Z.; investigation, E.S.Z., R.M.S. and A.A.N.; resources, A.A.N.; data curation, R.M.S. and A.A.Z.; writing—original draft preparation, E.S.Z., R.M.S., A.A.Z. and A.A.N.; writing—review and editing, E.S.Z., R.M.S., A.A.Z. and A.A.N.; visualization, E.S.Z.; supervision, E.S.Z. and A.A.Z.; project administration, E.S.Z.; funding acquisition, E.S.Z. All authors have read and agreed to the published version of the manuscript.

Funding: This research was funded by the Russian Science Foundation, grant number 22-77-10036.

Data Availability Statement: The crystallographic information file (cif) has been deposited as CCDC 2261773 via the joint Cambridge Crystal Data Centre CCDC/FIZ Karlsruhe deposition service.

Acknowledgments: The technical support of St. Petersburg State University Resource Centres "XRD" and "Geomodel" (Vladimir V. Shilovskikh and Natalia Vlasenko) is gratefully acknowledged.

Conflicts of Interest: The authors declare no conflict of interest.

References

1. Beudant, F.S. Alunogène, sulfate d'alumine. In *Traité Élémentaire de Minéralogie*, 2nd ed.; 1832; pp. 488–492. Available online: https://gallica.bnf.fr/ark:/12148/bpt6k9690962z (accessed on 2 June 2023).
2. Košek, F.; Culka, A.; Žáček, V.; Laufek, F.; Škoda, R.; Jehlička, J. Native alunogen: A Raman spectroscopic study of a well-described specimen. *J. Mol. Struct.* **2018**, *1157*, 191–200. [CrossRef]
3. Bariand, P.; Cesbron, F.; Berthelon, J.-P. Les sulfates de fer de Saghand près de Yazd (Iran). *Mémoire Hors-Série Société Géologique Fr.* **1977**, *8*, 77–85.
4. Biagioni, C.; Mauro, D.; Pasero, M. Sulfates from the pyrite ore deposits of the Apuan Alps (Tuscany, Italy): A review. *Minerals* **2020**, *10*, 1092. [CrossRef]
5. Zhitova, E.S.; Siidra, O.I.; Belakovsky, D.I.; Shilovskikh, V.V.; Nuzhdaev, A.A.; Ismagilova, R.M. Ammoniovoltaite, $(NH_4)_2Fe^{2+}{}_5Fe^{3+}{}_3Al(SO_4)_{12}(H_2O)_{18}$, a new mineral from the Severo-Kambalny geothermal field, Kamchatka, Russia. *Mineral. Mag.* **2018**, *82*, 1057–1077. [CrossRef]
6. Menchetti, S.; Sabelli, C. Alunogen. Its structure and twinning. *Tschermaks Mineral. Petrogr. Mitt.* **1974**, *21*, 164–178. [CrossRef]
7. Larsen, E.S.; Steiger, G. Dehydration and optical studies of alunogen, nontronite and griffithite. *Am. J. Sci.* **1928**, *15*, 1–19. [CrossRef]
8. Gordon, S.G. Results of the Chilean mineralogical expedition of 1938. Part VII. The crystallography of alunogen, meta-alunogen and pickeringite. *Not. Nat. Acad. Nat. Sci. Phila.* **1942**, *101*, 1–9.
9. Forti, P.; Panzica La Manna, M.; Rossi, A. The peculiar mineralogic site of the Alum cave (Vulcano, Sicily). In Proceedings of the 7th International Symposium on Vulcano Speleology, Canary Islands, Spain, 4 November 1994; pp. 35–44.
10. Fang, J.H.; Robinson, P.D. Alunogen, $Al_2(H_2O)_{12}(SO_4)_3{\cdot}5H_2O$: Its atomic arrangement and water content. *Am. Mineral.* **1976**, *61*, 311–317.
11. Sun, X.; Sun, Y.; Yu, J. Crystal structure of aluminum sulfate hexadecahydrate and its morphology. *Cryst. Res. Technol.* **2015**, *50*, 293–298. [CrossRef]
12. Krivovichev, S.V. Crystal chemistry of selenates with mineral-like structures. I. $(Al(H_2O)_6)_2(SeO_4)_3(H_2O)_4$—The selenate analog of alunogen. *Zapiski RMO* **2006**, *135*, 106–113. (In Russian)
13. Bibring, J.-P.; Langevin, Y.; Mustard, J.F.; Poulet, F.; Arvidson, R.; Gendrin, A.; Gondet, B.; Mangold, N.; Pinet, P.; Forget, F. Global mineralogical and aqueous Mars history derived from OMEGA/Mars express data. *Science* **2006**, *312*, 400–404. [CrossRef] [PubMed]
14. Swayze, G.A.; Ehlmann, B.L.; Milliken, R.E.; Poulet, F.; Wray, J.J.; Rye, R.O.; Clark, R.N.; Desborough, G.A.; Crowley, J.K.; Gondet, B.; et al. Discovery of the acid-sulfate mineral alunite in Terra Sirenum, Mars, using MRO CRISM: Possible evidence for acid-saline lacustrine deposits? In *EoS Transactions of the American Geophysical Union*; Fall Meeting Supplement; 2008; Volume 89, Abstract P44A-04. Available online: https://ui.adsabs.harvard.edu/abs/2008AGUFM.P44A..04S/abstract (accessed on 2 June 2023).
15. Kounaves, S.P.; Hecht, M.H.; Kapit, J.; Quinn, R.C.; Catling, D.C.; Clark, B.C.; Ming, D.W.; Gospodinova, K.; Hredzak, P.; McElhoney, K.; et al. Soluble sulphate in the martian soil at the Phoenix landing site. *Geophys. Res. Lett.* **2010**, *37*, L09201. [CrossRef]
16. Bish, D.L.; Blake, D.F.; Vaniman, D.T.; Chipera, S.J.; Morris, R.V.; Ming, D.W.; Treiman, A.H.; Sarrazin, P.; Morrison, S.M.; Downs, R.T.; et al. X-ray diffraction results from Mars Science Laboratory: Mineralogy of Rocknest at Gale Crater. *Science* **2013**, *341*, 1238932. [CrossRef]
17. Kahlenberg, V.; Braun, D.E.; Orlova, M. Investigations on alunogen under Mars-relevant temperature conditions: An example for a single-crystal-to-single-crystal phase transition. *Am. Mineral.* **2015**, *100*, 2548–2558. [CrossRef]

18. Kahlenberg, V.; Braun, D.E.; Krüger, H.; Schmidmair, D.; Orlova, M. Temperature-and moisture-dependent studies on alunogen and the crystal structure of meta-alunogen determined from laboratory powder diffraction data. *Phys. Chem. Miner.* **2017**, *44*, 95–107. [CrossRef]
19. Zhitova, E.S.; Khanin, D.A.; Nuzhdaev, A.A.; Nazarova, M.A.; Ismagilova, R.M.; Shilovskikh, V.V.; Kupchinenko, A.N.; Kuznetsov, R.A.; Zhegunov, P.S. Efflorescent Sulphates with M^{+} and M^{2+} Cations from Fumarole and Active Geothermal Fields of Mutnovsky Volcano (Kamchatka, Russia). *Minerals* **2022**, *12*, 600. [CrossRef]
20. Zhitova, E.S.; Sheveleva, R.M.; Zolotarev, A.A.; Krivovichev, S.V.; Shilovskikh, V.V.; Nuzhdaev, A.A.; Nazarova, M.A. The crystal structure of magnesian halotrichite, $(Fe,Mg)Al_2(SO_4)_4{\cdot}22H_2O$: Hydrogen bonding, geometrical parameters and structural complexity. *J. Geosci.* **2023**, accepted.
21. Sheveleva, R.M.; Nazarova, M.A.; Nuzhdaev, A.A.; Zhegunov, P.S.; Zhitova, E.S. Distribution and chemical composition of halotrichite from the geothermal fields of Kamchatka. Bulletin of Kamchatka Regional Association Educational-Scientific Center. *Earth Sci.* 2023, *accepted*. (In Russian)
22. Vakin, E.A.; Dekusar, Z.B.; Serezhnikov, A.I.; Spichenkova, M.V. The hydrothermal occurrences of the Koshelevskii volcanic massif. In *Hydrothermal Systems and Thermal Fields in Kamchatka*; Sugrobov, V.M., Ed.; DVNTs AN SSSR: Vladivostok, Russia, 1976; pp. 58–84. (In Russian)
23. Kalacheva, E.G.; Rychagov, S.N.; Koroleva, G.P.; Nuzhdaev, A.A. The Geochemistry of Steam Hydrothermal Occurrences in the Koshelev Volcanic Massif, Southern Kamchatka. *J. Volcanol. Seismol.* **2016**, *3*, 41–56. [CrossRef]
24. Balić-Žunić, T.; Garavelli, A.; Jakobsson, S.P.; Jonasson, K.; Katerinopoulos, A.; Kyriakopoulos, K.; Acquafredda, P. Fumarolic minerals: An overview of active European volcanoes. In *Updates in Volcanology, from Volcano Modelling to Volcano Geology*; Nemeth, K., Ed.; InTech: Rijeka, Croatia, 2016; pp. 267–322.
25. Kruszewski, Ł. Supergene sulphate minerals from the burning coal mining dumps in the Upper Silesian Coal Basin, South Poland. *Int. J. Coal Geol.* **2013**, *105*, 91–109. [CrossRef]
26. *CrysAlisPro Software System, Version 1.171.38.46*; Rigaku Oxford Diffraction: Oxford, UK, 2015.
27. Sheldrick, G.M. Crystal structure refinement with SHELXL. *Acta Crystallogr. A* **2015**, *71*, 3–8. [CrossRef] [PubMed]
28. Dolomanov, O.V.; Bourhis, L.J.; Gildea, R.J.; Howard, J.A.; Puschmann, H. OLEX2: A complete structure solution, refinement and analysis program. *J. Appl. Crystallogr.* **2009**, *42*, 339–341. [CrossRef]
29. Krivovichev, S. Topological complexity of crystal structures: Quantitative approach. *Acta Crystallogr. A* **2012**, *68*, 393–398. [CrossRef]
30. Krivovichev, S.V. Structural complexity of minerals: Information storage and processing in the mineral world. *Mineral. Mag.* **2013**, *77*, 275–326. [CrossRef]
31. Krivovichev, S.V. Structural complexity of minerals and mineral parageneses: Information and its evolution in the mineral world. In *Highlights in Mineralogical Crystallography*; Armbruster, T., Danisi., R.M., Eds.; Walter de Gruyter GmbH: Berlin, Germany, 2016; Volume 1, pp. 31–73.
32. Blatov, V.A.; Shevchenko, A.P.; Proserpio, D.M. Applied topological analysis of crystal structures with the program package ToposPro. *Cryst. Growth Des.* **2014**, *14*, 3576–3586. [CrossRef]
33. Jeffrey, G.A.; Jeffrey, G.A. *An Introduction to Hydrogen Bonding*; Oxford University Press: New York, NY, USA, 1997; Volume 12, pp. 1–228.
34. Pirajno, F.; Van Kranendonk, M.J. Review of hydrothermal processes and systems on Earth and implications for Martian analogues. *Aust. J. Earth Sci.* **2005**, *52*, 329–351. [CrossRef]
35. Zhitova, E.S.; Sergeeva, A.V.; Nuzhdaev, A.A.; Krzhizhanovskaya, M.G.; Chubarov, V.M. Tschermigite from thermal fields of Southern Kamchatka: High-temperature transformation and peculiarities of IR-spectrum. *Zapiski RMO* **2019**, *148*, 100–116.